2023

Quantifying geogrid reinforcement mechanism in roadway performance using Cyclic Plate Load (CPL) test

G.S. Ellithy
Embry-Riddle Aeronautical University

A. Crippa
Tenax Corportation

Geosynthetics: Leading the Way to a Resilient Planet – Biondi et al (eds)

Quantifying geogrid reinforcement mechanism in roadway performance using Cyclic Plate Load (CPL) test

G.S. Ellithy
Assistant Professor, Department of Civil Engineering, Embry-riddle Aeronautical University, Daytona Beach, FL, USA

A. Crippa
Vice President, Tenax Corporation, Baltimore, MD, USA

ABSTRACT: For decades, geogrids have been used successfully to improve performance in both paved and unpaved roadway construction. Even though the current state of practice differentiates between the design methodology incorporating geogrids in paved and unpaved roadways, the true improvement contribution of geogrids is to the base layer, or to the layer that is placed directly on top of it. It has been established that the three reinforcement mechanisms by which geogrids enhance roadway performance are: lateral restraint, bearing capacity increase and membrane tension support. In order to quantify these mechanisms and their contribution to the roadway performance improvement, two Cyclic Plate Load (CPL) tests were carried out, one on a paved section with a hot mix asphalt (HMA) top layer, and the second on an unpaved section. The tests included control and reinforced sections. Each test was instrumented with Linear Variable Differential Transducers (LVDTs) at the surface and subgrade levels that measured the displacements at these levels while the cyclic loads were applied. The paper presents the results in terms of the Reinforcement Improvement Ratio (RIR) which is calculated as the ratio between the number of load cycles of the reinforced section divided by the number of cycles of the control section at the same level of displacement. It was found that RIR is almost identical for surface displacements for both paved and unpaved roadway sections indicating the similar lateral restraint effect of the used product. The bearing capacity increase and membrane tension support vary between paved and unpaved sections depending on the level of displacement at the base course and subgrade contact. The results of those two tests were used to put an emphasis on quantifying the mechanism by which the geogrid contributes to the roadway performance improvement regardless whether it is paved or unpaved. The results could be used empirically to modify the current state of practice for geogrid contribution in paved and unpaved roadways. It should be noted that the terms soil *reinforcement* and soil *stabilization* have been used interchangeably to indicate the above soil improvements using geogrids.

1 INTRODUCTION

As stated by Holtz *et al.* (1998) When an aggregate layer is loaded by a wheel, the aggregate tends to move laterally, as shown in Figure 1a, unless it is restrained by the subgrade or a geosynthetic reinforcement layer. Soft, weak subgrade soils provide very little lateral restraint, so when the aggregate moves laterally, ruts develop on the aggregate surface and also in the subgrade. A geosynthetic layer with good interlocking capabilities, like a geogrid, or frictional ability like a geotextile, can provide tensile resistance to lateral aggregate movement. Bearing capacity increase is another geosynthetic reinforcement mechanism as shown in Figure 5-2b.

DOI: 10.1201/9781003386889-155

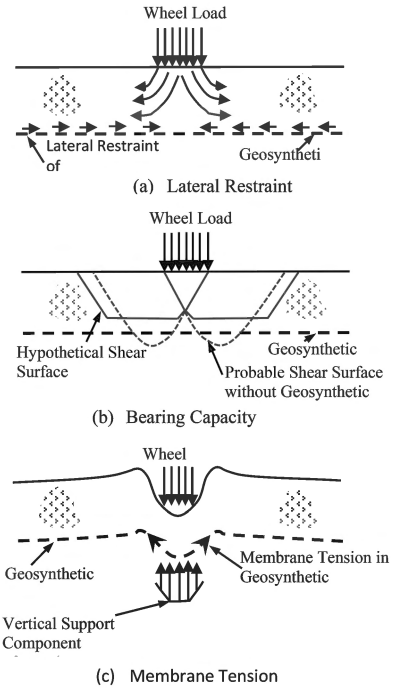

Figure 1. Possible reinforcement functions provided by geosynthetics in roadways: (a) lateral restraint, (b) bearing capacity increase, and (c) membrane tension support (after Haliburton, *et al*., 1981).

Similar to a footing, the use of geosynthetic reinforcement may force the potential bearing capacity failure surface to follow an alternate higher strength path. A third possible geosynthetic reinforcement function is membrane tension support of wheel loads, Figure 1c. In this case, the wheel load stresses must be great enough to cause plastic deformation and ruts in the subgrade. If the geosynthetic has a sufficiently high tensile modulus, tensile stresses will develop in the reinforcement, and the vertical component of this membrane stress will help support the applied wheel loads. Because tensile stress within the geosynthetic cannot be developed without some elongation, a significant rutting is needed to develop membrane-type support. Therefore, this mechanism is generally present in unpaved roads.

This paper presents the results from two Cyclic Plate Load (CPL) tests, one is performed on a paved section with a hot mix asphalt (HMA) top layer, and the second on an unpaved section. In both tests the California Bearing Ratio (CBR) of the subgrade was 2.0%. The testing conditions for the two tests were almost similar. Each test consisted of a control section and a reinforced section with the a geogrid layer placed on the subgrade where the base course layer was directly compacted on top of it. The tests were performed to investigate the geogrid reinforcement mechanisms in both paved and unpaved roadway sections and quantify these mechanisms if possible using the Reinforcement Improvement Ratio (RIR) which is calculated as the number of load cycles of the reinforced section divided by the number of load cycles of control section at the same displacement level.

2 CYCLIC PLATE LOAD (CPL) APPARATUS

The CPL test apparatus consisted of a rectangular concrete and steel test box that is 1.8 m deep, 2.3 m wide and 2.3 m long (6 ft × 7.5 ft × 7.5 ft). A stiff steel frame bolted to the top of the walls is used as a reaction for the servo-hydraulic actuator that provides the cyclic load to

the test surface. The servo-hydraulic system is programmed to continuously deliver individual load pulses having a trapezoidal shape and at a frequency of 1 Hz. The trapezoidal load pulse consists of four steps: ramp up to maximum load (0.3 s), hold maximum load (0.2 s), ramp down to minimum load (0.3 s), hold at minimum load (0.2 s). Max and min loads were 40 kN (9,000 lb) and 0.44 kN (100 lb), respectively, TRI (2019, 2022). The load was delivered to the road surface through a 2.5- cm (1-in). thick, 30- cm (12-in) diameter steel plate, designed to represent one equivalent single axle load (ESAL). Linear variable differential transducers (LVDTs) were positioned along the centerline of the load plate to measure vertical displacement of the surface as the test progressed, Figure 2. Information from these sensors was used to create a profile of the rut bowl resulting from the applied cyclic load. In addition, a single LVDT was also embedded in the subgrade to monitor displacement at the interface between the subgrade and base course (also the position of the geogrid for the reinforced tests). A data acquisition system was designed to monitor the applied load and displacement of all the LVDTs at a frequency of 25 Hz. From this data, a single max and min value was recorded for each of the sensors every 2 seconds.

Figure 2. Typical surface sensor setup.

3 MATERIAL PROPERTIES

3.1 *Subgrade*

The subgrade soil was classified as a lean clay with sand (CL) according to the USCS classification system, and had a liquid limit (LL) of 40% and Plasticity Index (PI) of 19%, with an optimum moisture content and dry density of 18.6% and 16 kN/m^3(101.4 lb/ft^3), respectively. Subgrade construction consisted of placing and compacting the subgrade material in six 15-cm (6-in) thick lifts in the CPL box. The subgrade was thoroughly mixed and moisture conditioned to ensure the subgrade was uniform when placed. The target shear strength for the subgrade was 86.5 $\pm$ 3 kPa to achieve a California Bearing Ratio (CBR) strength of 2.0 $\pm$ 0.1%. This strength corresponded to a moisture content of about 28%. In place shear strength was measured using a hand-held vane shear to ensure consistency and strength during construction. Compaction of the subgrade was accomplished using a jumping jack compactor. The sixth and final layer of the subgrade was leveled to a tolerance of $\pm$2.5 mm using a metal draw bar to cut the surface flat. The surface of the subgrade was covered with plastic during construction to prevent it from drying out.

3.2 *Geogrid*

A 3D structured geogrid was used in the reinforced test section. The geogrid in both tests was placed on the subgrade and the base course was compacted directly on top it. A single piece of geogrid was cut from the roll to fit within the width of the test box The material was cut out in a 45 degree orientation to allow instrumentation wires oriented in the machine and

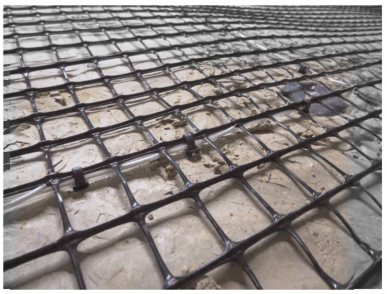

Figure 3. Geogrid instrumentation.

cross-machine directions to exit from the two front corners of the test box. The geogrid was pulled taut to remove any wrinkles and wooden stakes were used to hold the materials in place. A photo of the installed geogrid is shown in Figure 3.

3.3 *Base course*

The base course consisted of crushed granite, and has a gradation as shown in Figure 4. The base course was classified as poorly graded gravel (GP) according to the USACS. It was constructed in four lifts for a total depth of 30 cm (12 inches) and was compacted using a vibrating plate load compactor. The in-place density of the base course was measured using a sand cone device. The dry unit weight averaged 22 kN/m^3 (138 lb/ft^3). The strength CBR of the base course was verified using Dynamic Cone Penetrometer (DCP) and averaged 10%.

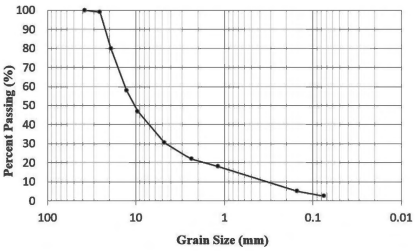

Figure 4. Grain size distribution for the base course.

3.4 *Hot Mix Asphalt (HMA)*

The hot-mix asphalt (HMA) used in the testing of the paved section was purchased from a local HMA plant and stored in steel drums. HMA was installed in two layers, by reheating the mix for each layer, screeding it to a uniform depth and compacting it using a flat vibrating plate compactor. The final mix averaged a density of 19.5 kN/m^3 (124 lb/ ft^3) and a depth of 5.7 cm (2.27 inches).

4 RESULTS AND DISCUSSION

Figure 5 shows the results of the first test which included a 5.7 cm HMA layer (paved section/ Test 1). The results are presented by comparing the number of load cycles corresponding to the same displacement for control and reinforced sections. The compared displacements are those occurring at the surface of the subgrade. The load cycles are compared for the subgrade surface displacement at about 6 mm (0.25 inch), and the Reinforcement

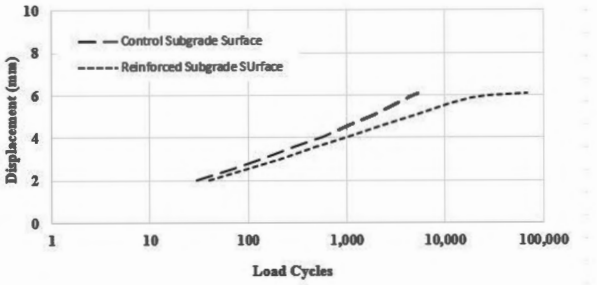

Figure 5. Subgrade surface displacement response for the paved section (Test 1).

Improvement Ratio (RIR) which is defined as the number of cycles for the reinforced section divided by the number of cycles of the control section, is about 13. An unexpected error occurred while measuring the displacement for the HMA surface and it is not presented in this comparison. As expected, the placement of a geogrid layer as a reinforcement inclusion between the subgrade and base course has significantly contributed to the performance of the paved section and increasing the number of load cycles, which could be translated to increasing design life.

Figure 6 shows the results of the second test which included a base course layer on top of the subgrade (unpaved section/ Test 2). Similar to the paved section, the results are presented by comparing the number of load cycles corresponding to the same displacement for control and reinforced sections. The compared displacements are those occurring at the surface of the base course and the surface of the subgrade. The load cycles are compared for the base course surface displacement at about 100 mm (4 inch), and the ratio is about 12. For the subgrade displacement which is at the level of 50 mm (2 inch), the ratio is also about 27. Similar to the paved section, the placement of a geogrid layer between the subgrade and base course has significantly contributed to increasing the number of load cycles, and hence design life.

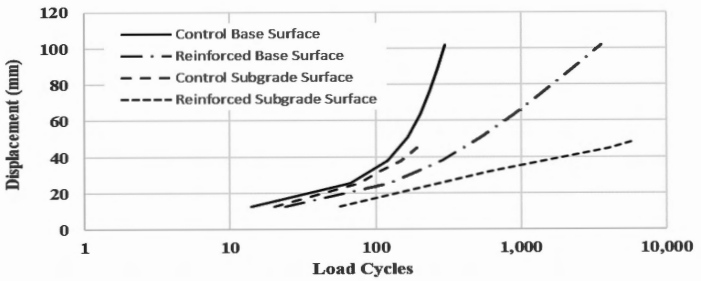

Figure 6. Base course and subgrade surface displacement response for the unpaved section (Test 2).

It is worth noticing the similarity between Test 1 and Test 2 RIR for the top surface displacements; top of subgrade in Test 1 (RIR = 13) and top of base course in Test 2 (RIR = 12), this indicates that for a given reinforcement level, or a given geogrid or geosynthetic product, the effect is almost identical for the lateral confinement mechanism which is the main mechanism responsible for geogrid reinforcement whether an HMA layer is present or not.

It was observed that the reinforced section in both paved and unpaved sections experiences less heave along the contact between base course and subgrade beyond the deforming area, and hence increase the bearing capacity of the reinforced section. The level of bearing capacity increases different between the paved and unpaved sections. The displacement

along this contact was recorded and will be presented in the final submission of the paper to show the effect of bearing capacity increase mechanism as an effect of geogrid reinforcement.

It could be noticed that the membrane tension support mechanism is more dominant in the unpaved section (Test 2) where the RIR of the subgrade surface displacement is 27, higher than all other calculated RIR values. That is again, an expected result, but now it could be qualified and a clear contribution of the reinforcement through this mechanism can be quantified.

5 SUMMARY AND CONCLUSIONS

This paper summarizes the results from two Cyclic Plate Load (CPL) tests on two roadway sections. Test 1 was on a paved section that included a 5.7- cm thick HMA layer on top of 30- cm thick base course overlying a 2% CBR subgrade. Test 2 was on an unpaved section with configuration similar to Test 1 but without the HMA layer. In both tests, a 3D geogrid was placed at the contact between the base course and the subgrade. To quantify the three mechanisms of reinforcement; lateral restraint, increase in bearing capacity and membrane tension support, results were presented in form of a ratio between the number of load cycles of the reinforced section to that of the control section at the same level of displacement. This ratio is referred to as the Reinforcement Improvement Ratio or RIR. The RIR was calculated for the top surface, top of HMA for Test 1 and top of base course for Test 2, and for top of subgrade for both tests.

It was found that RIR is almost identical for surface displacements for both paved and unpaved roadway sections indicating similar base course lateral restraint effect of the 3D geogrid used in the tests whether the section is paved or unpaved. The bearing capacity increase mechanism varied between paved and unpaved sections depending on the level of displacement at the base course and subgrade contact beyond the deforming area. More data will be presented at the final submission of the paper with regard to this mechanism. RIR of the subgrade surface displacement in Test 2 (unpaved) was 27, higher than all other calculated RIR values. This indicates that the membrane tension support mechanism is more dominant in unpaved sections where high level of displacement leads to elongation in the geogrid which in return increases the resistance to further displacement.

The results of those two tests were used to put an emphasis on quantifying the reinforcement mechanisms by which the geogrid contributes to improvement of roadway performance whether it is paved or unpaved. The results could be used empirically to modify the current state of practice for geogrid contribution in paved and unpaved roadways.

ACKNOWLEDGEMENT

The author would like to acknowledge TRI Environmental for providing the data of the tests discussed in this paper.

REFERENCES

Han, J. & Asce P.E. (2022) *Experimentally and Mechanistically Quantifying Benefits of Geosynthetics in Improved Road Performance*. Keynote Lectures, Eurogeo 7, Warsaw, Poland.

Holtz, R.D., Christopher, B.R., Berg, R.R. (1998) *Geosynthetics Design and Construction Guidelines*. FHWA HI-95-038

Haliburton, T.A., Lawmaster, I.D. & McGuffey, V.C. (1981) *Use of Engineering Fabrics in Transportation Related Applications*, FHWA DTFH61-80-C-Q0094.

TRI Environmental (2019) *Cyclic Plate Load Testing of Geosynthetic Reinforced Pavement Test Sections*. MAPP-LSM 2019-109

TRI Environmental (2022) *Cyclic Plate Load Test*. MAPP-LSM 2022-002.